

Electronic structure of titania nanosheets with vacancies based on first-principles calculations

Yuichi UCHIDA¹, Masahiro HARA¹, Asami FUNATSU² and Fuyuki SHIMOJO¹

¹*Department of Physics, Kumamoto University, Kumamoto 860-8555*

²*Department of Chemistry, Kumamoto University, Kumamoto 860-8555*

(Received May 31, 2017)

Titania nanosheets (TNSs) are expected to lead to higher photocatalytic performance than bulk TiO₂ because its high reactivity arises from the two-dimensional structure. Since physical properties of two-dimensional materials are susceptible to vacancies, it is essential to examine effects of vacancies on the electronic states of TNSs. In this study, we have investigated the electronic structures of TNSs with various types of vacancies based on first-principles calculations. It is confirmed that single-bonded oxygen atoms around a Ti vacancy greatly contribute to a bandgap narrowing and have high reactivity. In addition, it is suggested that the accurate discussion about the TNS with large-area vacancies requires the first-principles simulations using a larger system because Ti atoms around the large-area vacancies make bonds with adjacent Ti atom over the periodic boundary condition.

§1. Introduction

Titanium dioxide (titania, TiO₂) photocatalysts have been intensively researched because they have two valuable photocatalytic properties associated with ultraviolet absorption. One is their harmful substance decomposition function. When TiO₂ is photoexcited, excited electrons reduce oxygen and generate superoxide anions, while holes oxidize water and generate hydroxyl radicals.¹⁾ Since these reactive oxygen species have stronger oxidation power, materials coated with TiO₂ obtain antibacterial and deodorizing effects. The other important property of TiO₂ is super-hydrophilic conversion, which was discovered in the course of the study of the harmful substance decomposition function. The following mechanism of this phenomenon has been suggested. First, oxygen vacancies are formed by ultraviolet absorption. Next, water molecules are adsorbed on the vacancy sites. Finally, new hydroxyl groups are produced, which is responsible for the highly hydrophilic conversions.²⁾ This super-hydrophilic conversion gives a self-cleaning effect to materials coated with TiO₂.

Particularly, titania nanosheets (TNSs) attract much interest recently. The TNSs exhibit high reactivity because their two-dimensional structure increases reactive sites.³⁾ In addition, TNSs allow us to design new lightweight, flexible and high-performance functional materials because their thinness permits them to laminate other films. For example, an enhancement of the photochemical activity in layer-by-layer integration of TNSs and reduced graphene oxides has been reported.⁴⁾ For these reasons, it has been considered that TNSs have strong possibilities as a

next-generation photocatalytic material.

The chemical formula of a lepidocrocite-type TNS which is synthesized by the delamination from a parent layered $\text{K}_{0.8}\text{Ti}_{1.73}\text{Li}_{0.27}\text{O}_4$ crystal is $\text{Ti}_{0.87}\text{O}_2$.⁵⁾ In this structure, single-bonded O atoms around Ti vacancies are partially desorbed for the termination, which has been found from a comparison of transmission electron microscopy (TEM) images with first-principles structural optimization calculations.⁶⁾ Effects of one Ti vacancy or one two-coordinated O atom vacancy in TNS on electronic structures have already been discussed. The former vacancy decreases bandgap energy, while the latter vacancy has little effect on the electronic structure.⁷⁾ However, it is unclear how the electronic states change when two single-bonded O atoms around a Ti vacancy are desorbed as described above or when O atoms around a Ti vacancy are terminated by H atoms. The examination of the electronic structure of TNSs with such various vacancies is very important to evaluate photocatalytic functions of TNS in even more details.

In this study, we have investigated the relationship between the atomic structure with vacancies and the electronic states of TNSs based on the first-principles calculations.

§2. Computational methods

Electronic states are calculated using the projector-augmented-wave (PAW) method⁸⁾ within the framework of the density functional theory (DFT) in which the generalized gradient approximation (GGA)⁹⁾ is used for the exchange-correlation energy. The plane-wave cutoff energies are 30 Ryd. and 250 Ryd for the electronic pseudo-wave functions and the pseudo-charge densities, respectively. The energy functional is minimized using an iterative scheme.¹⁰⁾¹¹⁾ We use the Γ point for Brillouin zone sampling. As valence electrons, we include the 3d and 4s electrons of Ti (4 valence electrons), and 2s and 2p electrons of O (6 valence electrons), and 1s electron of H (1 valence electron). Other electrons in the lower energy electronic states of each atom are treated with the frozen-core approximation. Molecular dynamics (MD) simulations are carried out at 300 K, as controlled by a Nosé-Hoover thermostat.¹²⁾ The equations of motion for atoms are solved numerically using an explicit reversible integrator¹³⁾ with a time step of 1.21 fs. Whole computation time is 1.21 ps. The DFT plus Hubbard U model (DFT+ U) is employed in our calculation with $U_{\text{eff}} = 4.2 \text{ eV}$ ¹⁴⁾ to reproduce the on-site Coulomb interaction of localized d-electrons of Ti atoms.

In our calculations, the monolayer TNSs have been used in a $3 \times 3 \times 1$ supercell ($\text{Ti}_{18}\text{O}_{36}$, with a dimension of $11.445 \times 9.248 \times 10.00 \text{ \AA}^3$), as shown in Fig. 1(a), under periodic boundary conditions. We introduce a vacuum region in the z direction to disregard an interaction between TNSs. TNSs have two types of O sites. One is coordinated to two Ti atoms and labeled as O_{su} , and the other is coordinated to four Ti atoms and labeled as O_{in} (Fig. 1(b)).

We use a perfect TNS (Fig. 2(a)) and three electrically neutral TNSs with vacancies (Fig. 2(b)-(d)). Figure 2(b) shows the optimized structure in which the Ti2 is removed and O atoms around the Ti2 atom (O_1 , O_2 , O_4 , and O_5) are terminated by

H atoms (named TiV-H model). Figure 2(c) shows the optimized structure in which the Ti2, O1, and O2 atoms are removed (named TiO2upV model). Figure 2(d) shows the optimized structure in which the Ti2, O6, and O7 atoms are removed (named TiO2downV model).

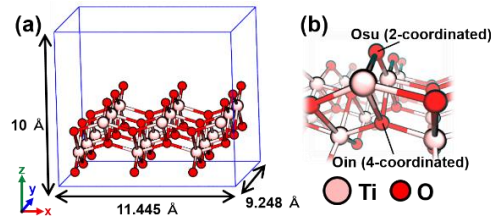


Fig. 1. A simulation cell (a) and a snapshot of two O sites (b). The large pink and middle red spheres indicate Ti and O atoms, respectively. Osu and Oin atoms are coordinated to two and four Ti atoms, respectively.

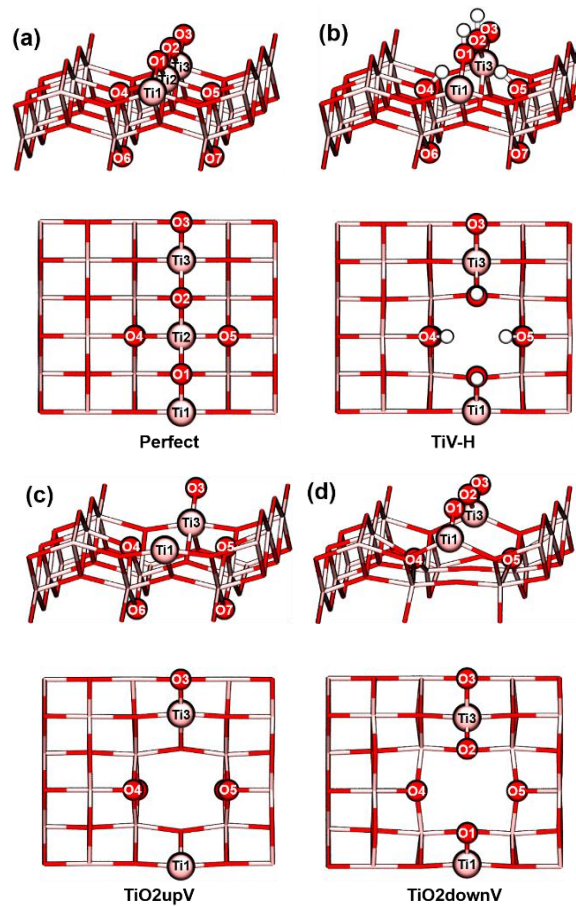


Fig. 2. Side (Top panels) and top (Bottom panels) views of snapshots of optimized structures in (a) the Perfect model (There are no vacancies), (b) the TiV-H model (Ti2 atom is removed and O atoms around the Ti2 vacancy are terminated by H), (c) the TiO2upV model (Ti2, O1, and O2 atoms are removed) and (d) the TiO2downV model (Ti2, O6, and O7 atoms are removed). The large pink, middle red, and small white spheres indicate Ti, O, and H atoms, respectively.

§3. Results and discussion

3.1. Electronic density of states and bandgap energy

Electronic density of states (DOS) and bandgap energy have been calculated for each TNS model using the results of MD simulations at 300 K (Fig. 3 and Table 1). It is confirmed that all TNSs are intrinsic semiconductors because the Fermi level exists in the middle between the valence band and the conduction band with small bandgap energies (< 3.5 eV). In addition, both electronic DOS and bandgap energies of the Perfect and TiV-H models correspond to each other because there are no dangling bonds in both the models. On the other hand, the bandgap energies of the TiO2upV and TiO2downV models are smaller than that of the Perfect TNS, and there is a clear difference in the electronic DOS. In the TiO2upV model, it is considered that since the electronic state energy levels around the Ti1 and Ti3 atoms shift downward, the bandgap reduction occurs. In the TiO2downV model, the bandgap narrowing is ascribed to the localized electronic states around the O1 and O2 atoms.

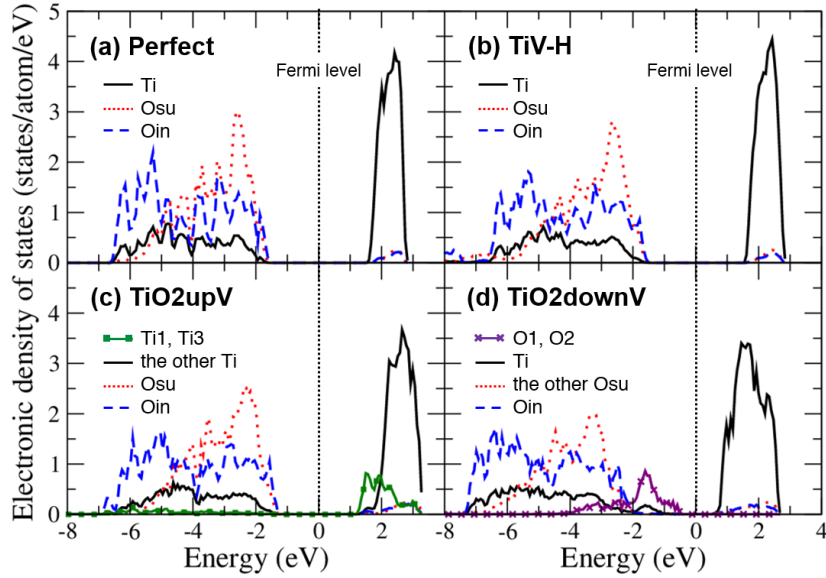


Fig. 3. Partial electronic density of states for (a) Perfect, (b) TiV-H, (c) TiO2upV, and (d) TiO2downV models.

	Perfect	TiV-H	TiO2upV	TiO2downV
Bandgap energy (eV)	3.49	3.46	2.91	1.69

Table 1. Calculated bandgap energies in the models studied.

3.2. Spatial distribution of electronic wave function

To clarify the electronic structure of TNSs in details, we have visualized wave functions for the highest occupied molecular orbitals (HOMOs) and the lowest unoccupied molecular orbitals (LUMOs), as shown in Fig. 4. It is confirmed that in both the Perfect and TiV-H model, HOMO and LUMO are mainly composed of 2p orbital of O atoms and 3d orbital of Ti atoms, respectively. This is consistent with the correspondence of the bandgap energy and DOS between the Perfect and the TiV-H models. In the LUMO snapshot for the TiO₂upV model, we see that bonding orbitals are formed between the Ti1 and Ti3 atoms over the periodic boundary condition in the y direction because the bonding of the same sign wave functions is formed. Since there are larger-area vacancies in the TiO₂upV model compared with any other models, a large structural relaxation occurs easily and leads to the formation of the bonding orbitals between the Ti1 and Ti3 atoms. Hence, it is considered that the electronic LUMO state around the Ti1 and Ti3 atoms is stabilized and leads to the bandgap narrowing. However, since this result would depend on the cell size, it is expected that the first-principles calculations using a larger system is needed to evaluate the electronic structure properly. In the HOMO snapshot for the TiO₂downV model, it is confirmed that HOMO is mainly composed of electronic states localized around the O1 and O2 atoms because these atoms have dangling bonds. Therefore, the bandgap reduction occurs in the TiO₂downV model.

In the Perfect model, the O1 and O2 atoms are coordinated to two Ti atoms, while the O4 and O5 atoms are coordinated to four Ti atoms. Thus, the effects of the Ti2-O4 or Ti2-O5 bond breaking would be smaller than those of the Ti2-O1 or Ti2-O2 bond. This is the reason why the electronic states of dangling bonds around the O4 and O5 are not localized.

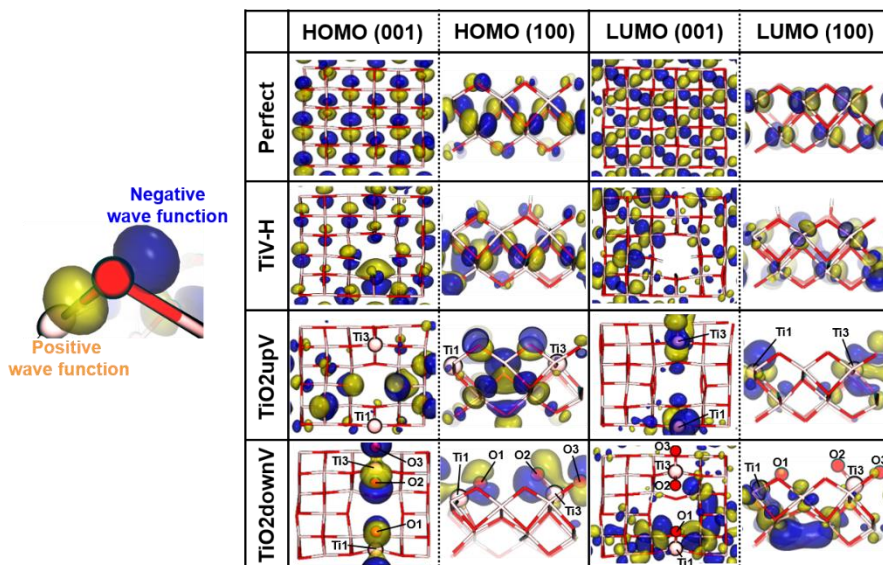


Fig. 4. Snapshots of atomic configurations and visualized wave functions of HOMOs and LUMOs at 1.21ps. They are taken in the [001] and [100] directions.

§4. Summary

In this study, the electronic structure of TNSs with vacancies has been investigated by using first-principles MD simulations. It has been confirmed that the electronic structure of TiV-H model corresponds with that of the Perfect model for the most part because there are no dangling bonds in the TiV-H model. It is verified that single-bonded oxygen atoms around a Ti vacancy greatly contribute to a bandgap narrowing and have high reactivity. In addition, we suggested that the accurate discussion about the TiO₂upV model requires the first-principle simulation using larger system because Ti atoms around the Ti vacancy make bonds with adjacent Ti atom atoms over the periodic boundary condition.

Acknowledgments

We would like to thank the Supercomputer Center, Institute for Solid State Physics, University of Tokyo for the use of facilities. The computations were also carried out the computer facilities at the Research Institute for Information Technology, Kyushu University.

References

- 1) M. R. Hoffmann, S. T. Martin, W. Choi, and D. W. Bahnemann, *Chem. Rev.* **95** (1995), 69.
- 2) N. Sakai, A. Fujishima, T. Watanabe, and K. Hashimoto, *J. Phys. Chem. B* **105** (2001), 3023.
- 3) N. Sakai, Y. Ebina, K. Takada, and T. Sasaki, *J. Am. Chem. Soc.* **126** (2004), 5851.
- 4) N. Sakai, K. Kamanaka, and T. Sasaki, *J. Phys. Chem. C* **120** (2016), 23944.
- 5) T. Sasaki, F. Kooli, M. Iida, Y. Michiue, S. Takenouchi, Y. Yajima, F. Izumi, B. C. Chakoumakos, and M. Watanabe, *Chem. Mater.* **10** (1998), 4123.
- 6) M. Ohwada, K. Kimoto, T. Mizoguchi, Y. Ebina, and T. Sasaki, *Scientific Reports.* **3** (2013), 2801.
- 7) C. Sun, T. Liao, G. O. Lu, and S. C. Smith, *J. Phys. Chem. C* **116** (2012), 2477.
- 8) P. E. Blöchl, *Phys. Rev. B* **50** (1994), 17953.
- 9) J. P. Perdew, K. Burke, and M. Ernzerhof, *Phys. Rev. Lett.* **77** (1996), 3865.
- 10) G. Kresse and J. Hafner, *Phys. Rev. B* **49**, (1994) 14251
- 11) F. Shimojo, R. K. Kalia, A. Nakano, and P. Vashishta, *Comput. Phys. Commun.* **140**, (2001) 303.
- 12) W. G. Hoover, *Phys. Rev. A* **31** (1985), 1695.
- 13) M. Tuckerman, B. J. Berne, and G. J. Martyna, *J. Chem. Phys.* **97** (1992), 1990.
- 14) B. J. Morgan and G. W. Watson, *Surf. Sci.* **601** (2007), 5034.